EXPERIMENTAL STUDY ON MECHANICAL PROPERTIES OF ALUMINUM ALLOYS UNDER UNIAXIAL TENSILE TESTS

Olfa Daghfas[1][*], Amna Znaidi[1], Ahmed Ben Mohamed[1], Rachid Nasri[1]

[1]*National Engineering School of Tunis El Manar University, Laboratory of Applied Mechanics And Engineering (LMAI), BP 37, Le Belvedere 1002 Tunis, Tunisia*

ABSTRACT

The 7075 aluminum alloy (a typical Al–Zn–Mg–Cu alloy) is one of the most important engineering alloys. It is mainly used in the automotive industry, in transport and aeronautics, due to its excellent strength/weight ratio. The purpose of the present research is to model the behavior of 7075 aluminum alloy and to build an experimental database to identify the model parameters. Firstly, the paper presents an experimental device of simple tensile tests and the studied material on 7075 aluminum alloy. Thus, uniaxial tensile tests are carried out in three loading directions relative to the rolling direction. From experimental hardening curves and Lankford coefficients, the mechanical properties are extracted, particularly the various fractures owing to pronounced anisotropy relating to the material. Secondly, plastic anisotropy is then modeled using the identification strategy which depends on yield criteria, hardening and evolution laws. By smoothing experimental hardening curves in the tensile tests, a selection is made in order to choose the most appropriate hardening law for the identification of the studied material. Finally, a comparison with experimental data shows that the behavior model can successfully describe the anisotropy of the Lankford coefficient.

Keywords: Aluminum alloy; Experimental uniaxial tensile test; Hardening law; Lankford coefficient; Mechanical properties

1. INTRODUCTION

The study of the behavior of metallic materials during the forming process is an important subject. The nature of the used materials and solicitations require a formulation taking into account elastoplastic behavior, finite deformation and the anisotropy of the material, in particular for thin sheet metal forming (Kim et al., 2000). Despite the importance of the work in this field, aluminum alloys continue to be the center of interests of several types of research in materials science. Their use in the automotive and aviation industry depends largely on their mechanical and thermal characteristics. The addition of zinc in aluminum does not alter the mechanical properties. Therefore, metallurgists have turned to ternary aluminum-zinc-magnesium alloys (with or without copper) of the 7000 series that have been widely used as structural materials, due to their attractive comprehensive properties, such as low density, high strength, ductility, toughness, and resistance to fatigue (Yespica, 2012; Xiaobo, 2016).

The 7075 aluminum alloy (a typical Al–Zn–Mg–Cu alloy) is one of the most important engineering alloys. It is mainly used in the automotive industry, in transport and aeronautics, due to its excellent strength/weight ratio (Williams, 2003). These alloys have very good

mechanical properties; it is the high-strength aluminum alloys with a low resistance to corrosion. The mechanical strength of these alloys is increased by the structural hardening phenomenon (Dursun & Soutis, 2014). This type of alloy is mainly used in the automotive industry, in transport and aeronautics, especially in the design of the fuselage of the Airbus (Pham, 2015).

Sheet metals or plates are obtained by hot and cold rolling which creates plastic anisotropy. Thus, they have a particular texture, characterized by a preferred orientation of the grains constituting the material (Lee et al., 2009). This texture gives the sheet a special plastic behavior. The plastic behavior is well described by a load surface which evolves during the plastic deformation for different tests. Mechanical properties and plastic behavior give rise to certain properties from the processing of aluminum alloy sheet especially cold rolling. These have been reported by many authors from several different mechanical experiments. These experiments include tensile tests (Barlat et al., 1991), pure shear tests (Gilmour et al., 2001) and combined loading tests (Lesuer, 2000) on specimens with several geometries (bar, plate, sheet).

Recently, various types of research on aluminum alloy are focused on mechanical properties, texture and anisotropic behavior that give rise to certain properties from the processing of aluminum alloy sheet (Boumaiza, 2008; Lee et al., 2009; Tajally & Emadoddin, 2011). For modeling the plastic behavior, two aspects of the anisotropy are taken into account: the initial anisotropy due to the initial texture of the metal sheets and the anisotropy induced by cold working (Ben Mohamed et al., 2016), mainly due to the development of dislocation structures in the material (Dogui, 1989; Boumaiza, 2008).

There has been little research on formability and anisotropic behavior of commercialized 7075 aluminum alloy. However, the influences of loading orientations on aluminum alloy plate are still an open question.

The aims and objectives of the present study are to describe and characterize the mechanical properties, the anisotropic behavior of high-strength aluminum alloy loaded at 0°, 45°and 90° to the rolling direction of the 3 mm thick plate, and to provide direction for obtaining the optimized parameters for 7075 aluminum alloy in metal forming. As the initial anisotropy is taken into account through a yield criterion (Dogui, 1989), the Yld91 anisotropic yield function proposed by Barlat et al. (1991) is chosen to model the elastoplastic behavior of the 7075-T7 aluminum alloy. The plastic parameters were determined using an experimental database from uniaxial tensile tests. Numerical simulations of the experimental tensile tests were performed using the anisotropic elastoplastic model. Predicted stress-strain curves were in very good agreement with the experimental curves for three loading directions. The results of the simple tensile tests were used subsequently to show the evolution of Lankford coefficient and load surface for several tests.

2. EXPERIMENTAL PROCEDURE

2.1. Material

The 7075 aluminum alloy with structural hardening, which is a thinly rolled sheet with a thickness of 3 mm, is used. The chemical composition according to EN 573 standard is shown in Table 1.

Table 1 Chemical compositions of 7075-T7 (Barralis &Maede, 1995)

S_i	C_u	M_n	M_g	C_r	Zn	Ti	Fe	Al
0.5	4.9	0.9	1.8	0.1	0.25	0.15	0.5	remainder

In this study, the used alloy in state T7351 is subsequently referred to as 7075-T7. Table 2 presents the heat treatment applied to the 7075 alloy.

2.2. Dimensions and Form of the Test Specimens

The uniaxial test is ensured by a specific geometry defined by the standard NF A 03-151 (Develay, 1990). The schematic tensile specimen used for this study is shown in Figure 1. The current dimensions of the useful part are $L_0 = 50$ mm and $b_0 = 12.5$ mm, respectively.

The specimens are cut in three directions relative to the rolling direction (RD) in the plane of the sheet (see Figure 2a). In the following description, the rolling direction is referred to as RD, the transverse direction as TD and the direction (45° from the RD) as DD. The angle between the loading and the rolling directions will be noted subsequently ψ.

Three samples were prepared for each loading direction to verify repeatability.

2.3. Experimental Set

The test is carried out using a hydraulic press (SHIMADZU) that has a maximum load capacity of 30 kN (Figure 2c), class 0.5 BS EN ISO-1. A chain acquisition (see Figure 2d) allows recording of the strain as a function of stress. The loading speed is 4MPa.s-1. Two electronic extensometers are used to measure the strain rate according to the width and the thickness along the tensile test (Figure 2b).
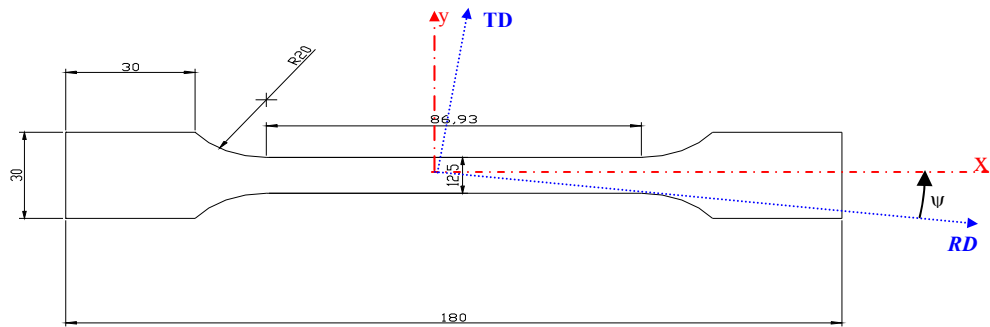

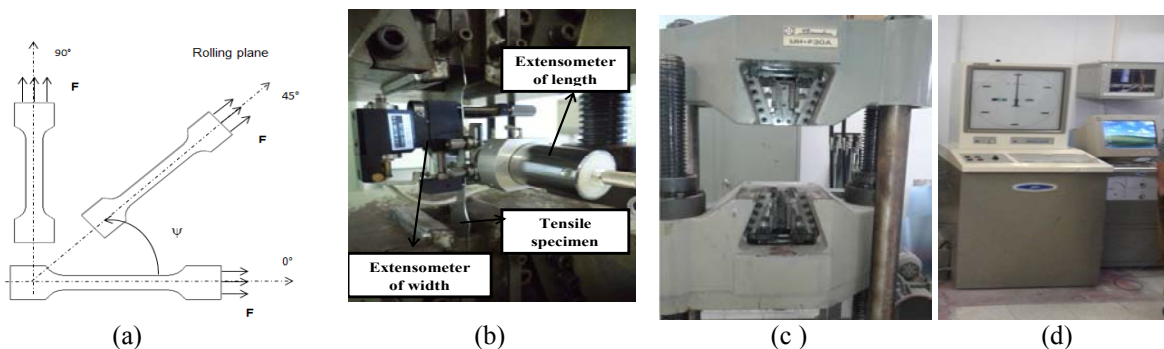Figure 1 Tensile specimen used in the present study, the useful area ($L_0 = 50$ mm, $b_0 = 12.5$ mm)

| (a) | (b) | (c) | (d) |

Figure 2 (a) Loading Direction of cutting; (b) Electronic extensometer; (c) Tensile test machine; and (d) acquisition chain (LGM)

2.4. Experimental Results

The experimental database contains three tensile curves and their experimental Lankford coefficients. Experimental tensile curves of 7075-T7 in three directions 0°(RD), 45°(DD), and 90°(TD) from the rolling direction are presented in Figure 3.

Figure 3 shows similar yield strength and plastic deformation characteristics in the rolled RD and the 45° direction until 11.5% in strain. The TD direction has a similar yield strength, but

different hardening characteristics and lower elongation (8%). This result exhibits a marked tensile anisotropy where strengths and ductility vary with orientation in the plane of the sheet. The 7075 in temper T7 is defined by maximum percentage elongation along the rolling direction and minimum value along the transverse direction.
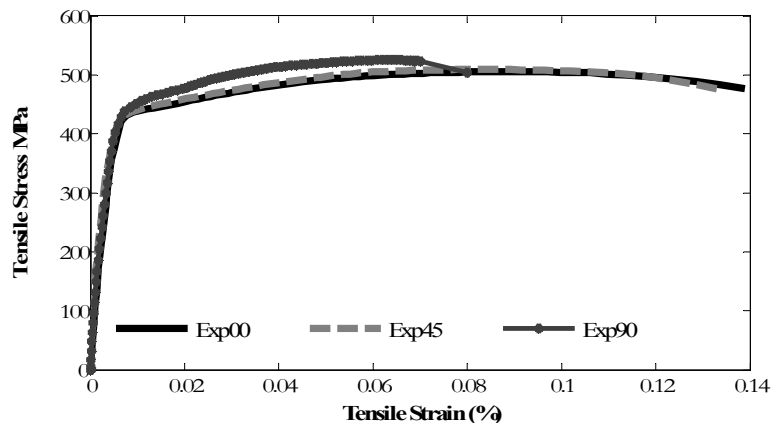

Figure 3 Experimental tensile curves obtained at 0°, 45° and 90° to RD

Maximum yield Re and tensile Rm strengths are observed especially in the transverse direction, but a significant decrease in percentage elongation A%. This is explained by the structural hardening.

The commercialized aluminum alloy 7075 in T7 temper is much stronger than pure Aluminum A5 (Znaidi et al, 2016) (around a 40 MPa compared to a 430 MPa for the yield strength), but it has a failure percentage elongation A% (maximum plastic deformation of 0.13 against 0.27 for pure aluminum).

According to the experimental results, we are seeing the influence of the anisotropy on the specimen fracture especially after transverse loading (90°).

Table 3 shows the experimental Lankford coefficients relating to three loading directions.

Table3 Experimental Lankford coefficient for different loading directions

ψ	$r(\psi)$
00°	0.069
45°	0.138
90°	0.099

The anisotropy coefficient illustrates the deformation mode of the metal sheet. A small Lankford Coefficients indicated by 7075-T7 led to a significant reduction in thickness.

The tensile test is the simplest and most widely used because it allows obtaining a lot of information (elastic modulus, yield strength, maximum load, elongation at the break) and maintaining a homogeneous strain in the useful parts.

2.5. Anisotropic Elastoplastic Model

This work is limited to plastic orthotropic behavior. The materials are treated as incompressible with negligible elastic deformations. Models are formulated for standard generalized materials with an isotropic hardening described by an internal hardening variable, a law of evolution and an equivalent deformation. The material is initially orthotropic and remains orthotropic;

isotropic hardening is assumed to be captured by a single scalar internal hardening variable denoted by ε^p.

The behavior model is defined by:

2.5.1. Yield function

In particular, we will assume that the elastic range evolves homothetically, the yield criterion is then written as follows in Equation 1:

$$f\left(q,\varepsilon^p\right) = \sigma_{_.}\left(q\right) - \sigma_{_.}\left(\varepsilon^p\right) \leq 0 \tag{1}$$

σ_c : Equivalent stress is given by the Barlat criterion as shown in Equation 2:

$$\sigma_c\left(q\right) = \left(\left|q_1 - q_2\right|^m + \left|q_2 - q_3\right|^m + \left|q_1 - q_3\right|^m\right)^{1/m} \tag{2}$$

where $q_{k=1,2,3}$ are the eigenvalues of a modified stress deviator tensor q defined as follows in Equation 3:

$$q = A : \sigma^D \tag{3}$$

σ^D is the deviator of the Cauchy stress tensor (incompressible plasticity).

The fourth order tensor A carries the anisotropy by 6 coefficients c_1, c_2, c_3, c_4, c_5, c_6.

$\sigma_s\left(\varepsilon^p\right)$: Isotropic hardening function; where ε^p is the equivalent plastic strain.

2.5.2. Hardening law

Using as a hardening function respectively as described in Hollomon, Voce (1948) and Bron's (2004) laws as shown in Equations 4, 5, and 6:

Hollomon's Law

$$\sigma_s\left(\varepsilon^p\right) = K\left(\varepsilon^p\right)^n \tag{4}$$

K and *n* is the Hollomon parameters to identify.

Voce's Law

$$\sigma_s\left(\varepsilon^p\right) = \sigma_s\left(1 - \alpha\exp\left(\beta\varepsilon^p\right)\right) \tag{5}$$

This law introduces a hardening saturation σ_s, α and β describe the non-linear part of the curve during the onset of plasticity where $0 < \alpha < 1$ and $\beta < 0$.

Bron's Law

This law is proposed by Bron, (2004) with six parameters to be identified.

$$\sigma_s\left(\varepsilon^p\right) = \sigma_0\left[1 + K_0\varepsilon^p + K_1\left(1 - \exp\left(-k_1\varepsilon^p\right)\right) + K_2\left(1 - \exp\left(-k_2\varepsilon^p\right)\right)\right] \tag{6}$$

It is a modified expression of Voce's Law and it contains twice the number of exponential expressions as shown in Equation 5.

σ_0 is the yield strength; K_0 and K_1 are the variables for hardening saturation; k_1 and k_2 describe the non-linear part of the hardening curve.

2.5.3. Evolution law

The direction of the plastic strain rate $\dot{\varepsilon}^p$ is perpendicular to the yield surface and is given by Equation 7:

$$\dot{\boldsymbol{\varepsilon}}^{\mathrm{p}} = \dot{\lambda}\,\frac{\partial \mathrm{f}}{\partial \boldsymbol{\sigma}^{\mathrm{D}}} \tag{7}$$

With λ plastic multiplier that can be determined from the consistency condition $\dot{\bar{\mathrm{f}}} = 0$.

2.5.4. Lankford Coefficient

In the characterization of thin sheets, the plastic anisotropy with different directions is frequently measured by the Lankford coefficient r_{ψ} that is given by the following expression shown in Equation 8:

$$\mathrm{r}_{\boldsymbol{\psi}} = \dot{\boldsymbol{\varepsilon}}_{\mathrm{yy}}\big/\dot{\boldsymbol{\varepsilon}}_{\mathrm{zz}} \tag{8}$$

where $\dot{\boldsymbol{\varepsilon}}_{\mathrm{yy}}$ and $\dot{\boldsymbol{\varepsilon}}_{\mathrm{zz}}$ are the plastic strain rates in-plane and through the thickness, respectively.

In the case of orthotropy $\mathrm{r}_{\boldsymbol{\psi}}$ varies depending on the off axis angle ψ. This scalar quantity is used extensively as an indicator of the formability.

3. RESULTS

In this section we focus on the phenomenology of plastic behavior; especially modeling plasticity and hardening based on experimental data represented as families of hardening curves and Lankford coefficient data. In order to simplify our identification process, the following assumptions are adopted:

In identification through the "small perturbations" process, the tests used are treated as homogeneous tests and we neglect the elastic deformation. The behavior is considered as being rigid plastic incompressible. Then the plasticity surface evolves homothetically (isotropic hardening) and all tests are performed in the plane of the sheet resulting in a plane stress condition.

The identification of this constitutive law requires the identification of the hardening function, the anisotropy coefficients. (While respecting the plane stress condition, the Barlat criterion parameters are reduced to 4 (c_1, c_2, c_3, c_4), the shape factor m and the Lankford coefficients $r(\psi)$.

3.1. Identification of the Hardening Laws

From the experimental results, the hardening curves are fitted using the three laws presented above. These curves allow us to determine the parameters of the different laws (see Table 2) and to choose the most appropriate law to describe the plastic behavior of the studied alloy.

The smoothing returns are shown in order to identify the parameters of the hardening laws, while minimizing the quadratic difference between the theoretical and experimental results. The classical hardening laws are apparent in the adjustment of their functions on experimental curves to identify the unknown parameters.

The identified curves shown by Hollomon's, Voce's and Bron's laws are compared to the experimental tensile curves obtained in the three loading directions relative to the rolling direction (0° and 45°), which are presented in Figure 4a and Figure 4b, respectively. Then a comparison is made in order to show the most suitable law for the identification of the hardening curves.

In order to show the most suitable law for the identification of tensile stress-tensile strain curves, a comparison between three hardening laws is made.

Figure 4 shows a net adjustment between the theoretical and experimental results particularly in the homogeneous part of the plastic deformation. A significant difference in results between the two laws is visible by zooming in on the curves. It is seen that in the plastic deformation part the Voce and the Bron laws describe the hardening curves better than Hollomon's Law for all loading directions from the rolling direction. After the necking zone, it is clear that Bron's Law or Voce's Law offers a better description. Voce's Law better describes the hardening curve. This is because of the exponential form that makes the law more adequate throughout the curves.

Table 2 Identification of the constants in the hardening laws for different loading directions

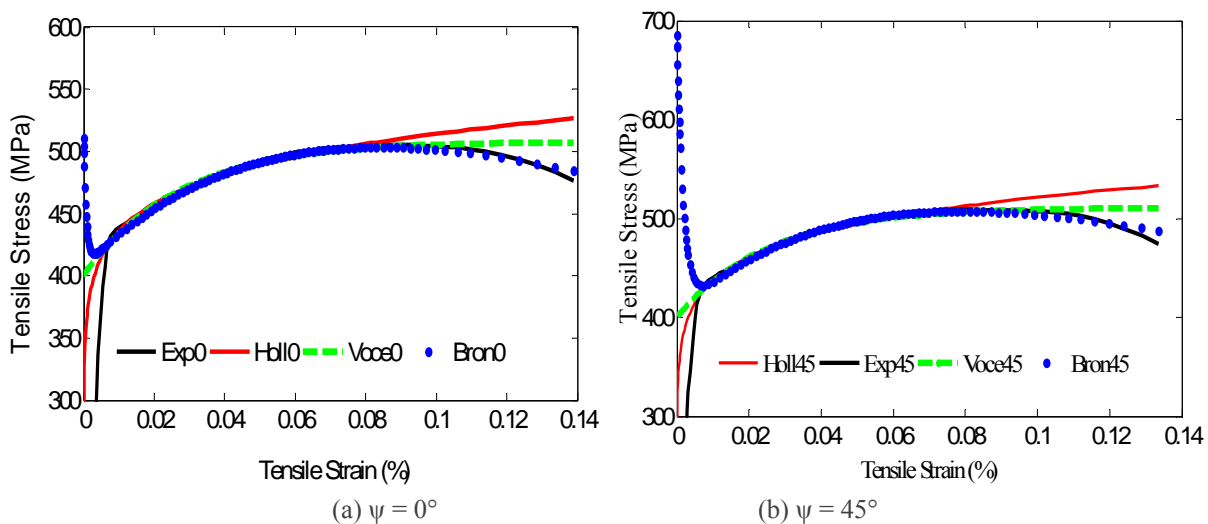| Laws	Parameters	0°	45°	90°
Hollomon	k	606.8441	622.0848	671.2648
	n	0.0718	0.0766	0.0853
Voce	σ_y	508.0623	511.1316	531.9995
	α	0.2111	0.2161	0.2613
	β	-36.8421	-39.3294	-49.5677
Bron	σ_0	514.3	685.6313	243.4389
	K_0	-2.1	-1.41558	-4.2122
	K_1	-0.2	-0.4097	0.7002
	K_2	1322.1	564.3529	461.7965
	k_1	0.5	0.3361	0.9195
	k_2	15.4	19.0331	24.5559

Figure 4 Identification of the hardening curve: (a) $\psi = 0°$; (b) $\psi = 45°$

By convention, Bron's Law with six parameters is selected subsequently to identify anisotropy behavior in the next work.
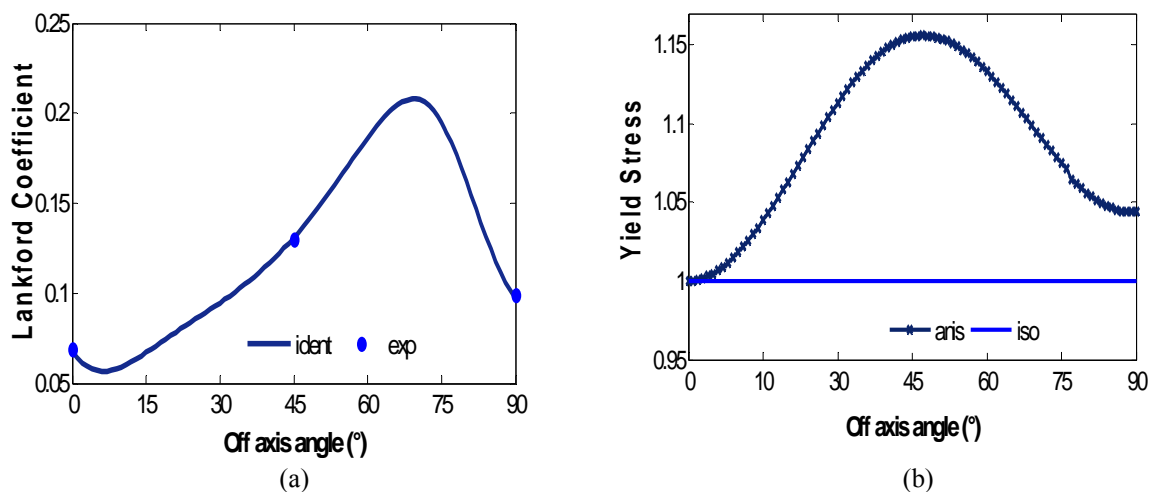
3.2.   Identification of Anisotropic Parameters

Using the simplex algorithm and using the non-quadratic Barlat criterion (2) and respecting the assumptions, the second step of the identification strategy is equivalent to choosing the coefficients of anisotropy (c_1, c_2, c_3, c_4) and the shape coefficient shown m (Table 6), while minimizing the squared difference between the theoretical and experimental results.

Table 6 Identification of anisotropic coefficients and a shape coefficient m

c_1	c_2	c_3	c_4	m
0.3612	0.3431	0.113	1.0539	6.2486

Using the identified anisotropic coefficients, the evolution of Lankford coefficient $r(\psi)$ and the anisotropy $\sigma(\psi)/\sigma_0$ based on off-axis angles ψ are presented in Figure 5a and Figure 5b, respectively.

Figure 5 (a) Evolution of Lankford coefficient; (b) Evolution of the yield stress anisotropy based ψ

A good agreement has been found between the experimental and predicted Lankford coefficients with respect to the rolling direction (see Figure 5a). Thus, the behavior model describes very satisfactorily the plastic behavior of this alloy because its yield function and its hardening law are suitable for aluminum alloys.

The evolution of anisotropy of 7075-T7 is more pronounced especially in a 45° direction from the rolling direction (see Figure 5b), therefore the 7075-T7 is more suitable for the forming process for the manufacture of the aerospace parts.

In order to avoid fracture during shaping of parts the direction of 45° is chosen for loading.

3.3. Validation
In order to validate the behavior model, the experimental tensile curve in the transverse direction and the identified anisotropic parameters of behavior model are used.

Figure 6 shows a good agreement between the theoretical results of the behaviorial model and the experimental data for transverse direction.

3.4. Evolution of the Yield Surface in Deviatory Plane $\left(\overline{x_2}, \overline{x_3}\right)$

After having identified and validated the behavior model, we will study the evolution of load surfaces for several tests and the stress anisotropy of the material.

Using the identified anisotropic coefficients (Table 2), the behaviorial model allows representation of the load surfaces on each test (simple tensile ST for $\theta = \pi/3$, simple shear SS for $\theta = \pi/2$, wide tensile WT for $\theta = \pi/6$) in the deviatory plan (Znaidi et al., 2016).

where

$$\begin{cases} \overline{x_2} = \left| \sigma^D \right| sin\,\theta\,cos\,2\psi \\ \overline{x_3} = \left| \sigma^D \right| sin\,\theta\,sin\,2\psi \end{cases} \tag{9}$$
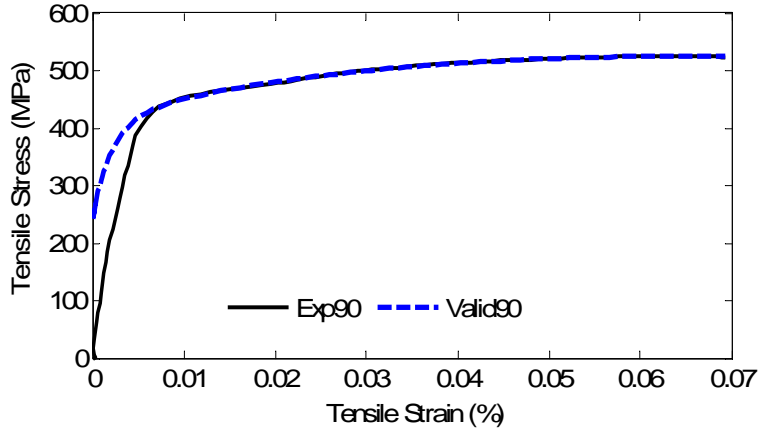

Figure 6 Validation of hardening tensile curve at $\psi = 90°$

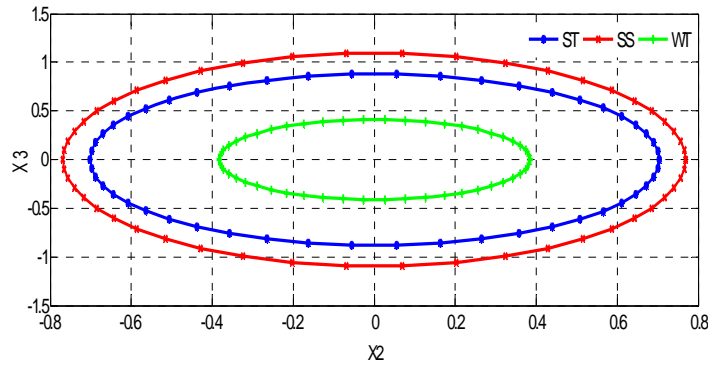Figure 7 shows the comparison between the yield surfaces calculated by behavior model on the different tests.

Figure 7 Evolution of the load surface in the deviatory plan $\left(\overline{x}_2, \overline{x}_3 \right)$

It appears also that this material is resistant to simple shear much more than simple tensile and wide tensile stress. Furthermore, for simple tensile and simple shear tests, the 7075-T7 alloy is plasticized quickly along the 45° direction from the rolling direction. In contrast, in wide tensile stress conditions, it is achieved at the same time as at three loading directions.

4. CONCLUSION

Since the commercial 7075 aluminum alloys are essentially aeronautics alloys, off-axis tensile tests were carried through three loading directions. These experimental results have allowed investigation of the mechanical properties and identification of the plastic behavior model using a proposed identification strategy. By comparing both experimental and calculated data based on Barlat criterion and Voce hardening law, it was demonstrated that this model leads to a good description and identification of the plastic behavior of the aluminum alloy in the uniaxial test. The results of the simple tensile test were subsequently used to show the evolution of load surface for several tests. It was deduced that the best shaping in the design of the fuselage is

realized using the 7075 alloy in the 45° direction. It is seen that this type of alloy has important mechanical strengths, but low percentage elongation. To remedy this disadvantage a succession of thermo-mechanical treatments will be applied to this commercial aluminum alloy. This latter point presents a topic for the next research.

5. ACKNOWLEDGEMENT

6. REFERENCES

Barlat, F., Lege, D.J., Brem, J.C., 1991. A Six-component Yield Function for Anisotropic Materials. *International Journal of Plasticity*, Volume 7, pp. 693–712

Barralis, S.J., Maede, R.G., 1995. *Specific-Metallurgy-Development, Structures, Properties Normalization.* AFNOR, NATHAN

Ben Mohamed, A., Znaidi, A., Daghfas, O., Nasri, R., 2016. Evolution of Mechanical Behavior of Aluminum Alloy Al 7075 during the Time of Maturation. *International Journal of Technology*, Volume 7(6), pp. 1076–1084

Boumaiza, A., 2008. Influence of Structural Anisotropy of the Plastic Behavior during Deformation by Stamping. *Ph.D. Thesis* at the University Mentouri, Constantine

Bron, F., 2004. Ductile Tearing Thin 2024 Aluminum Alloy Sheets for Aeronautical Application. *Ph.D. Thesis*, National School of Mines of Paris, (MINES ParisTech)

Daghfas, O., Znaidi, A., Nasri, R., 2015. Numerical Simulation of a Biaxial Tensile Test Applied to an Aluminum Alloy 2024. *In*: The 6th International Conference on Advances in Mechanical Engineering and Mechanics. Hammamet, 20–22 December 2015, Tunisia

Develay, R., 1990. *Properties of Aluminum and Aluminum Alloys*. Technical Engineer, M440

Dogui, A., 1989. Anisotropic Plasticity in Large Deformation. *Ph.D. Thesis* of Sciences, University Claude Bernard-Lyon I

Dursun, T., Soutis, C., 2015. Recent Developments in Advanced Aircraft Aluminium Alloys. *Materials and Design*, Volume 56, pp. 862–871

Gilmour, K.R., Leacock, A.G., Ashbridge, M.T.J., 2001. The Determination of the in-plane Shear Characteristics of Aluminum Alloys. *Journal of Testing and Evaluation*, Volume 29, pp. 131–137

Kim, J.M., Yang, D.Y., Yoon, J.W., Barlat, F., 2000. The Effect of Plastic Anisotropy on Compressive Instability in Sheet Metal Forming. *International Journal of Plasticity*, Volume 16, pp. 649–676

Lee, N.S., Chen, J.H., Kao, P.W., Chang, L.W., Tseng, T.Y., Su, J.R., 2009. Anisotropic Tensile Ductility of Cold-rolled and Annealed Aluminum Alloy Sheet and the Beneficial Effect of Post-anneal Rolling. *Scripta Materialia*, Volume 60, pp. 340–343

Lesuer D.R., 2000. *Experimental Investigations of Material Models for Ti-6Al-4V Titanium and 2024-T3 Aluminum*, Report No. DOT/FAA/AR-00/25

Pham, T.T., 2015. Damage to the Surface of Aluminum Alloys in Cold Forming. *Ph.D. Thesis* in Science at the University Valenciennes, Hainautcambresis

Tajally, M., Emadoddin, E., 2011. Mechanical and Anisotropic Behaviors of 7075 Aluminum Alloy Sheets. *Materials & Design*, Volume 32(3), pp. 1594–1599

Voce, E., 1948. The Relationship between Stress and Strain for Homogeneous Deformations. *Journal of the Institute of Metals*, Volume 74, pp. 537–562

Williams, J.C., Starke, E.A., 2003. Progress in Structural Materials for Aerospace Systems. *Acta Materialia*, Volume 51, pp. 5775–5799

Xiaobo, Y., 2016. Fatigue Crack Growth of Alumina Alloy 7075-T651 under Non-proportional Mixed Mode I and Mode II Loads. *Frattura ed Integrità Strutturale*, Issue 38 pp. 148–154

Yespica, W.J.P., 2012. Comparative Study of the Electrochemical Behavior of 2024 -T351and 7075-T7351 Aluminum Alloys Neutral Sodium Sulfate Middle. *Ph.D. Thesis* in Science at Toulouse University

Znaidi, A., Daghfas, O., Gahbiche, A., Nasri, R., 2016. Identification Strategy of Anisotropic Behavior Laws: Application to Thin Sheets of A5. *Journal of Theoretical and Applied Mechanics*, Volume 54(4), pp. 1147–1156